



June 2020

*Prepared by Fasmatech & Karolinska Institute*

## CONTENTS

### D2.1 Protocol of in situ testing of the optimized ion isolation technique

<i>2.1.1 The Omnitrap Platform</i> .....	2
<i>2.1.2 AC waveform excitation</i> .....	3
<i>2.1.3 Resolving DC</i> .....	5
<i>2.1.4 RF Duty Cycle</i> .....	7
<i>2.1.5 Frequency Calibration</i> .....	8
<i>2.1.6 Summary</i> .....	10

## D2.1 Protocol of in situ testing of the optimized ion isolation technique

### 2.1.1 The Omnitrap Platform

A 3D CAD model of the Omnitrap platform is presented in **Figure 1**. The Omnitrap is a radio-frequency (RF) linear ion trap consisting of nine consecutive segments, three of which are active trapping regions sustaining a diverse ion activation network for processing ions. Ions are confined axially in purposed designed regions by controlling the DC profile applied across these segments while radial confinement is accomplished by a pair of anti-phase and frequency-adjustable rectangular RF waveforms. A set of gas pulse valves allows for fast thermalization of ions during storage or after transfer between the different regions. Resonance excitation of ions is performed in segments Q2 and Q5 by the application of AC waveforms enabling frequency sweep isolation and slow-heating collision induced dissociation. The RF poles in Q5 are designed with 2 mm apertures to facilitate external injection of electrons, neutrals and charged particles, while optical access for photo-dissociation experiments is available in Q8 and from the back end of the Omnitrap platform.

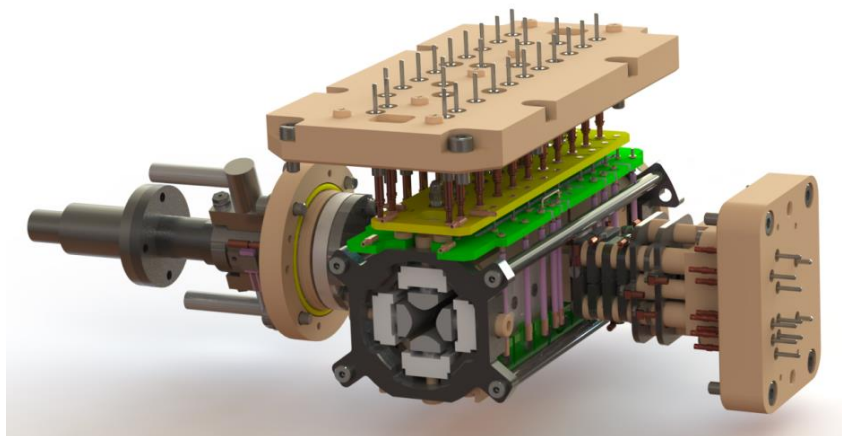


**Figure 1.** 3D CAD model of the Omnitrap platform highlighting the linear ion trap design including the multipin feedthru for distributing RF, AC and DC signals to all pole-electrodes of the system, the variable energy electron source and the thermal version of the hydrogen atom source.

The design of the Omnitrap platform enables multistage tandem mass spectrometry experiments to be performed with very high efficiency. In combination with ion accumulation, the storage and superposition of multiple sets of fragment ions prior to mass analysis, the quality of MS<sub>n</sub> spectra produced is far superior to existing analytical platforms. These features are uniquely suited for top down mass spectrometry where the overwhelming abundance of fragmentation channels of a precursor ion reduces the signal-to-noise ratio considerably. The tandem MS functionality is supported by ion isolation methods, which are the necessary intermediate steps between consecutive stages of ion activation.

The RC network for distributing the RF, AC and DC signals to the poles of the linear ion trap are shown in **Figure 2**. Individual DC switches are used to define the DC offset of each segment, while two separate

transformers are employed to superimpose the AC signal onto the two anti-phase rectangular RF waveforms in Q2 and Q5, respectively. The different methods available to perform ion isolation are also highlighted in **Figure 3**. These methods have been investigated experimentally and results are presented further below.

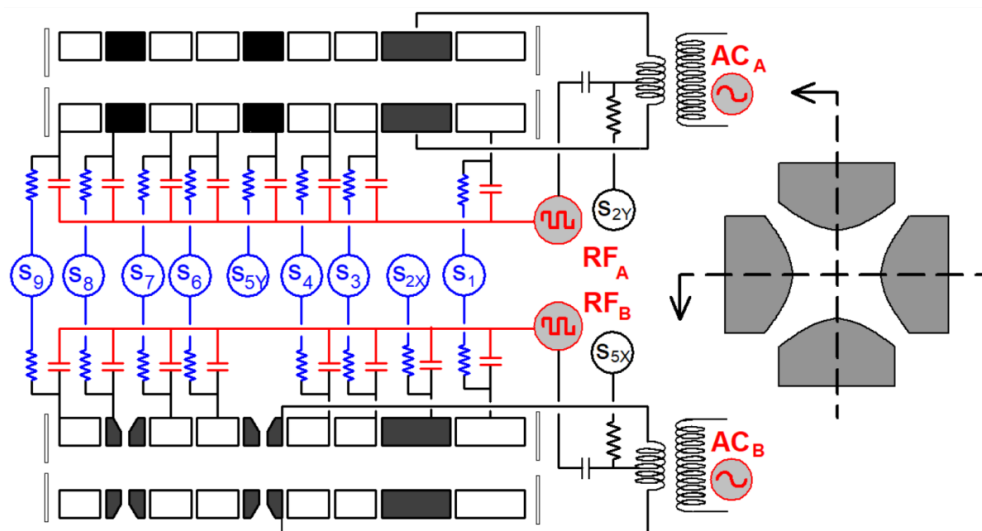


**Figure 2.** RC distribution network for RF, AC and DC signals applied to the poles of the Omnitrap platform.



**Figure 3.** The different ion isolation methods available in Q2 and Q5 include the application of AC waveforms, the application of a resolving DC similarly to the operation of a quadrupole mass filter as well as controlling the duty cycle of the rectangular RF waveforms.

### 2.1.2 AC waveform excitation

Sinusoidal RF waveforms allow for parking ions with different  $m/z$  ratios at the same  $q_z$  value through adjustments in the RF amplitude. Different ions located at the same position in the stability diagram will exhibit the same secular frequency. This property of sinusoidal RF waveforms allows for the application of a frequency sweep or other types of AC signals with a predetermined frequency notch. In contrast, ion parking in traps driven by rectangular RF waveforms is accomplished by adjusting frequency and as a result ions with different  $m/z$  ratios positioned at the same  $q_z$  value will exhibit different secular frequencies. Consequently, the notch of an AC signal employed for ion isolation varies across the  $m/z$  range of interest. This effect increases the demand for high speed communication protocols and advanced software algorithms for fast FFT calculations. To address this problem, the electronics, and the control software currently under development will be able to generate in real time frequency sweep and other types of AC

isolation waveforms (filtered noise field – FNF) with adjustable parameters. **Figure 4** shows an example of a frequency sweep isolation waveform designed with two notches and applied to the poles of segment Q2 in dipolar form to isolate two different charge states of the light chain fragment produced by CID of a monoclonal antibody (mAb). **Figure 5** shows the mass spectrum and the corresponding isolation windows.

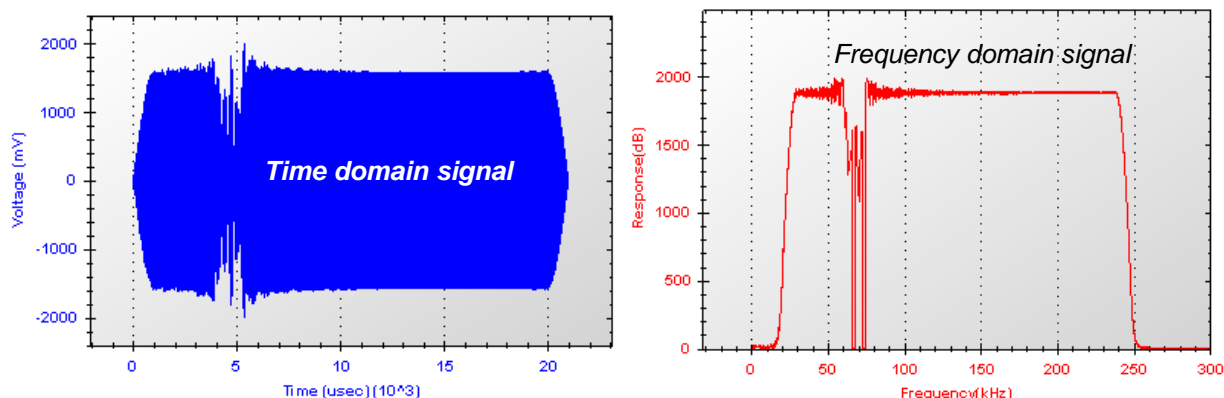


**Figure 4.** Frequency sweep AC signal designed with two notches shown in time and frequency domains.

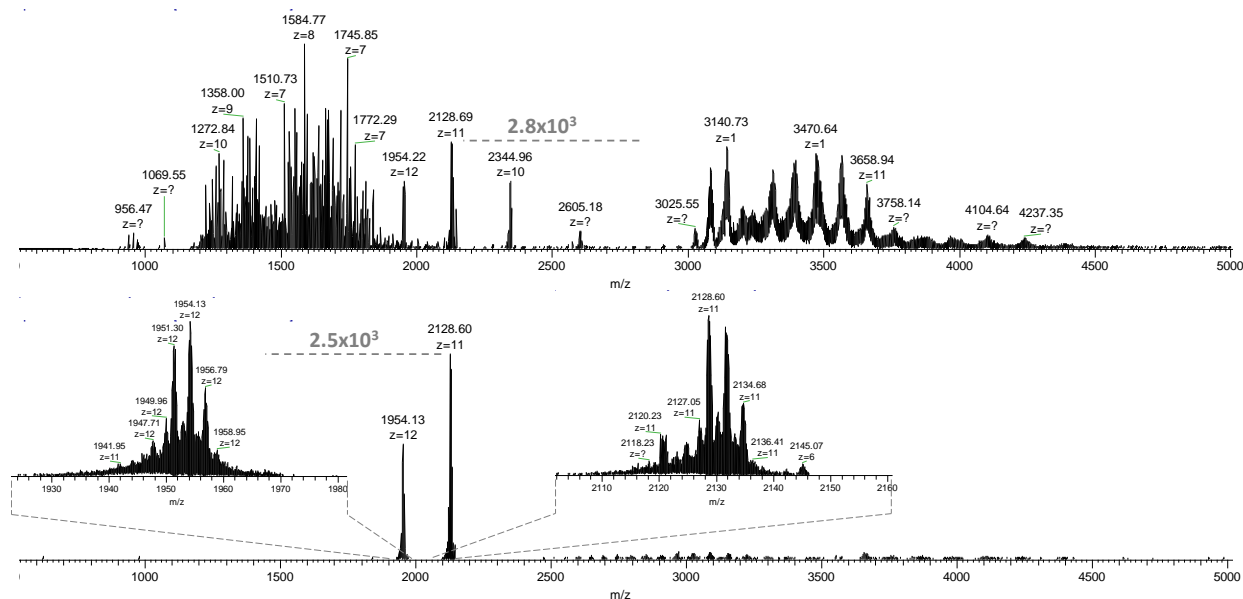


**Figure 5.** CID mass spectrum of intact Herceptin charge state 49+ and the isolation windows produced by the application of the multi-notch frequency sweep waveform shown in shown in Figure 4.

Several hardware and firmware upgrades are nearly completed that will allow for real time decision making, generation and application of AC waveforms. Improvements in the communication between the FPGA unit and the PC have been implemented based on USB3 technology. The FT601Q chip affords a 300MByte/s data bandwidth and a 20ms long AC waveform can be downloaded to the FPGA external DDR memory module within 2ms. Optimization of the source code developed for generating AC signals has been completed and the calculation time has been reduced to <30ms. Further optimization in the VHDL

language responsible for transferring the instruction sequence information for defining the experimental parameters dynamically has been completed. Overall, the hardware aspect of the necessary functionality for the real-time decision-making protocol is nearly completed, while several upper level software developments are underway. This includes the user interface for frequency calibration and automated application of multi-notched AC excitation/isolation waveforms. Finally, the API communication protocol between the Orbitrap mass spectrometer and the Omnitrap electronics has been finalized. **Figure 6** shows a block diagram describing the different modules and the flow of information for real-time decision-making, which will allow operating the Orbitrap-Omnitrap configuration in data dependent acquisition mode.

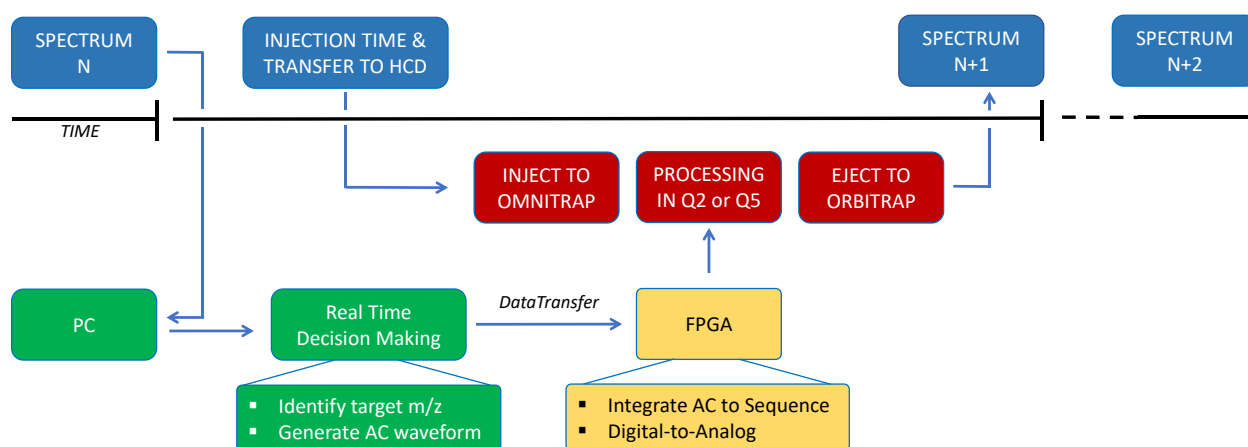


**Figure 6.** Block diagram for operating the instrument in data dependent acquisition mode.

All these developments are mostly related to the application of AC waveforms in real time, however, isolation using a resolving DC signal, which is currently the easiest and most efficient method in multistage tandem MS experiments, will also be implemented in a similar manner.

### 2.1.3 Resolving DC

Resolving DC signals are typically applied in quadrupole mass filters and  $m/z$  selection is performed during transmission of ions through the device. In the Omnitrap platform two opposite resolving DC potentials are applied to the poles of Q2 or Q5 while ions are confined axially by weak DC voltages applied to neighboring segments. **Figure 7** shows a typical sequence for receiving a wide range of  $m/z$  ratios in the trap, parking a specified  $m/z$  value at  $q=0.55$  and subsequently applying a pair of resolving DC potentials to change the slope of the operating line and park the ion of interest at the tip of the stability diagram. Ion trapping at the tip of the stability diagram is exercised for  $<1\text{ms}$  before the resolving DC signals is switched off.

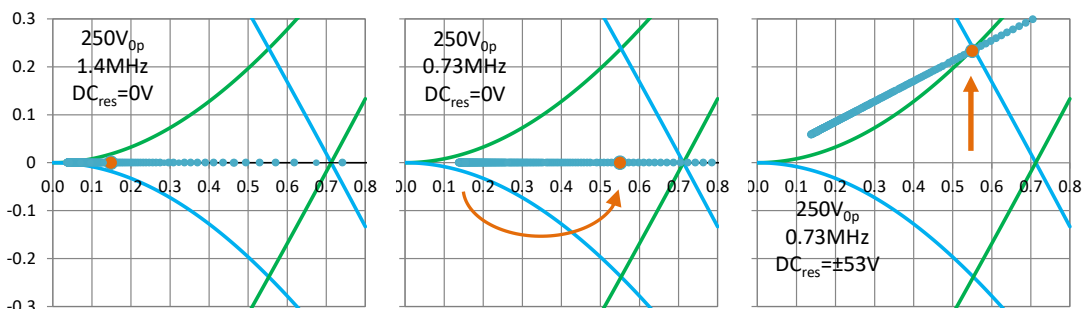


**Figure 7.** a-q stability diagrams for a linear ion trap with  $r=4\text{mm}$  driven by two antiphase rectangular RF waveforms. Ions with  $m/z=500$  are parked at  $q=0.55$  and ultimately at the tip of the stability diagram following the application of a resolving DC.

Mass spectra demonstrating resolving DC isolation of a single charge state of a monoclonal antibody electrosprayed under native conditions are presented in **Figure 8**. These experiments are performed in a Q-Exacte Plus upgraded with Biopharma option. The Omnitrap platform extends the isolation range far beyond the 3000<sup>th</sup> limit imposed by the electronics of the Q-Exacte. **Figure 9** summarizes resolving DC isolation results across a wide range of  $m/z$  values obtained experimentally and by using ion optical simulations. The resolution of this method can exceed 100 after careful tuning and without experiencing significant ion losses (>80% transmission). This resolution is sufficient for isolation of individual charge states of native and denatured mAbs but not high enough for isolation of specific glycosylated species. The calculated resolution required for isolating different glycoforms is 1,000, which for the current setup is greater by a factor of 5x compared to the resolution achievable with the frequency sweep method discussed above.

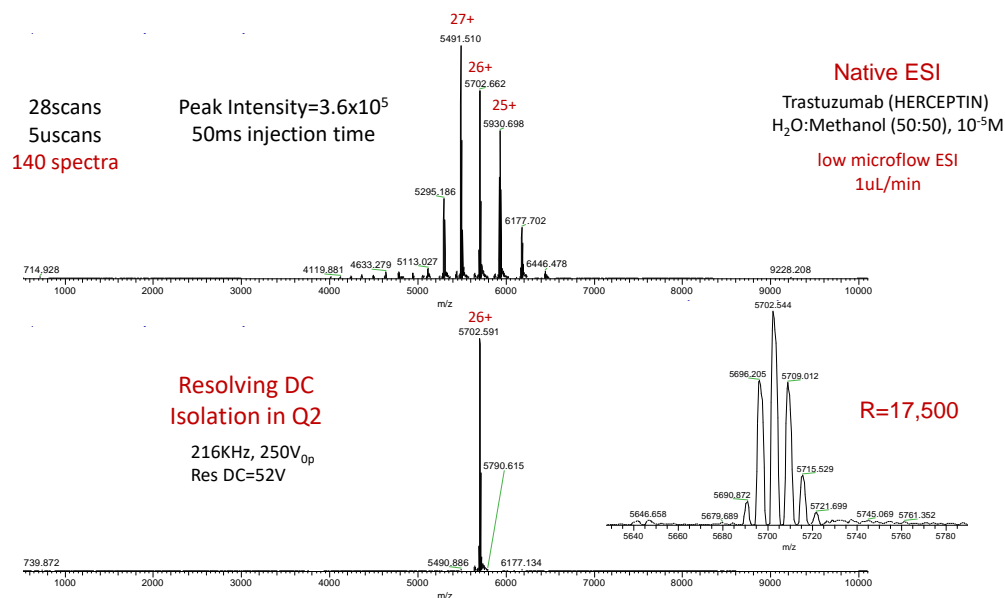


**Figure 8.** Mass spectrum of Herceptin sprayed under native conditions and resolving DC isolation of charge state 26+. The glycosylation profile is also highlighted.

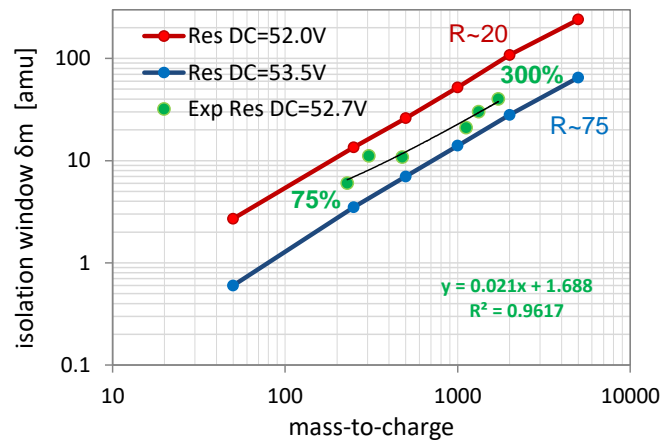


**Figure 9.** Width of the resolving DC isolation window across a wide range of  $m/z$  values determined experimentally and by ion optical. The RF amplitude is fixed at  $250V_{op}$ .

### 2.1.4 RF Duty Cycle

Yet another option available for ion isolation in the Omnitrap platform is the rotation of the stability diagram through variations in the duty cycle of the RF waveform. **Figure 10** shows the rotated stability diagram with a 60% duty cycle introduced to both anti-phase RF waveforms. Also shown are the two waveforms highlighting the balancing effect of the isolation capacitor and the additional resolving DC applied necessary to offset the RF amplitudes to  $\pm 250V_{op}$ . Experiments performed so far with protein ions and lower  $m/z$  fragment species have shown that the resolving DC method offers higher resolution and higher transmission compared to this approach.

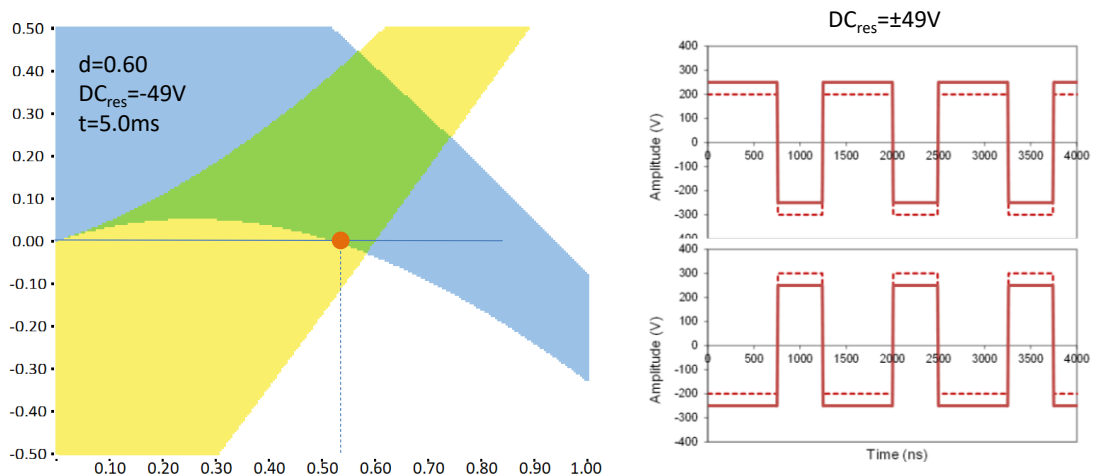


**Figure 10.** Rotation of the stability diagram using a 60% duty cycle and the anti-phase RF waveforms with the superimposed resolving DC component adjusted to offset the effect of the isolation capacitor.

### 2.1.5 Frequency Calibration

New software functionalities have been developed to determine the secular frequency of the ions across the entire range of  $q_z$  values in an automated manner. These calculations will be used to generate calibration curves and simplify the instruction sequence files developed by the user to operate the instrument. The purpose here is for the user to select the  $m/z$  value of interest only, while all necessary calculations for adjusting RF frequency, excitation frequency and amplitude are performed in the background. This work will be extended for real time decision making necessary for operating the instrument in DDA mode.

The user-interface is presented in **Figure 11**. The code is constructed to receive a list of definitions, for example the  $m/z$  values of interest, the position of the ions in the stability diagram determined by the value of  $q_z$ , the excitation amplitude, scan range, averaging parameters, convergence criteria etc. In brief, the RF frequency is calculated for a fixed value of  $m/z$  and  $q_z$ . The curve shown in **Figure 11** represents ion intensity as a function of the excitation frequency and the minimum corresponds to the secular frequency of the ion for a particular set of experimental conditions. Finally, a 3D plot is generated associating secular frequency to a corresponding RF frequency and  $q_z$  value. Such multi-dimensional calibration surfaces will be generated for a few different  $m/z$  ratios and different charge loads providing the necessary information to automate ion isolation, CID and ultimately develop the DDA mode. **Figure 12** shows the calculations steps undertaken to determine ion secular frequency experimentally.

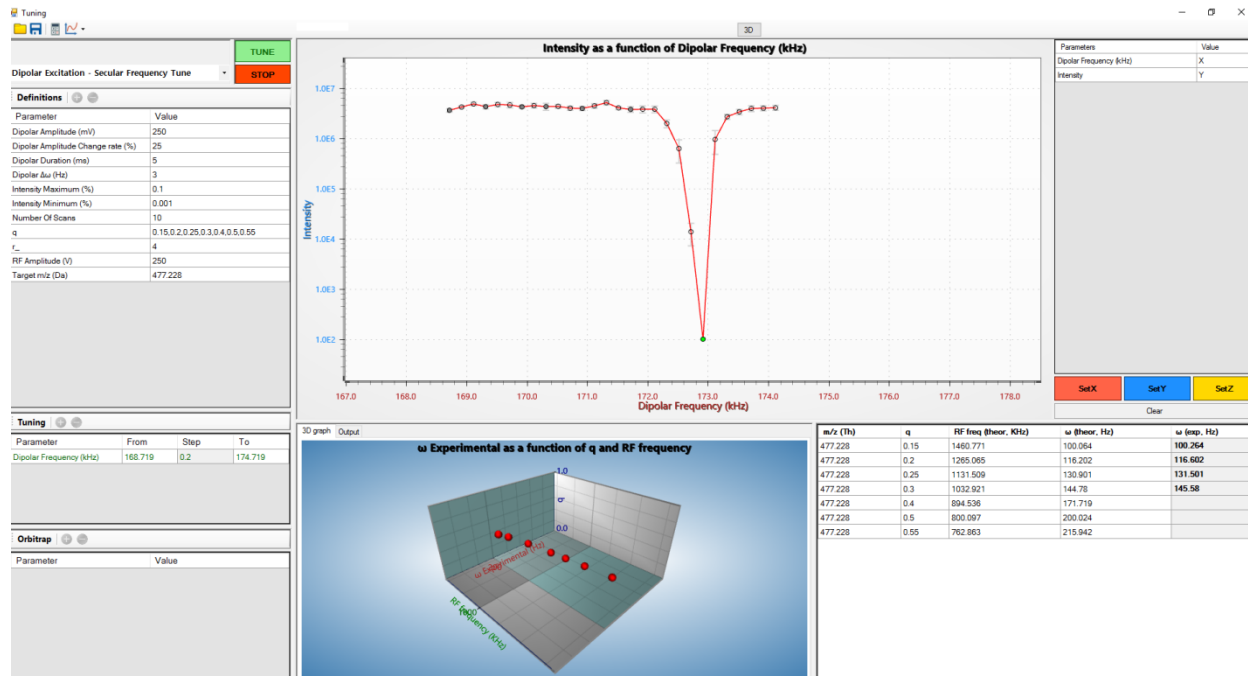


**Figure 11.** UI for automatic generation of calibration surfaces associating ion secular frequency to RF frequency and stability parameters.



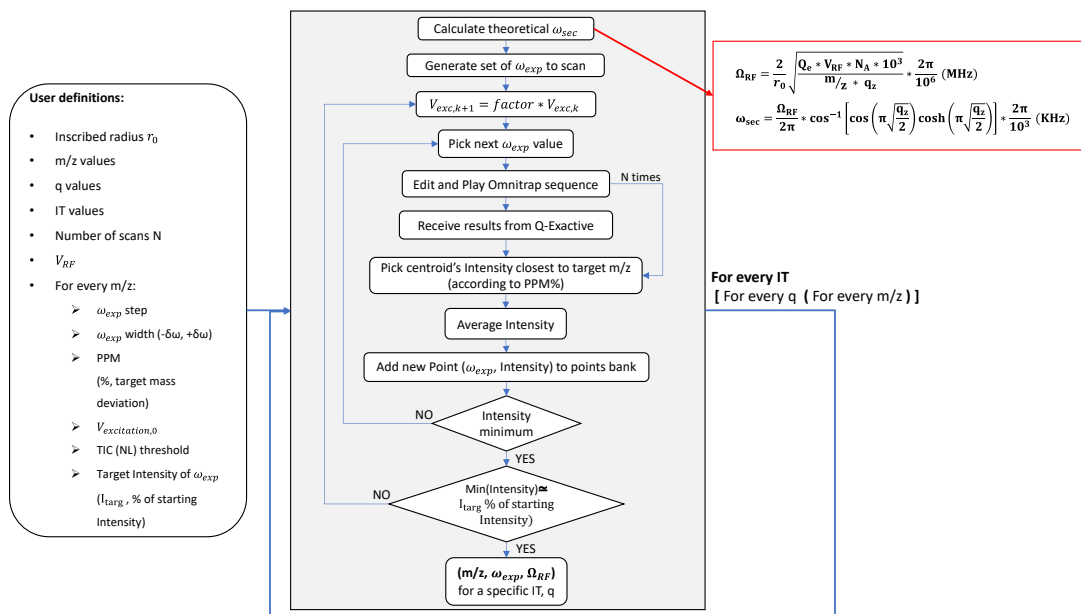


**Figure 12.** Calculation steps underlying the secular frequency calibration procedure described in Figure 11. Definitions and mathematical expression utilized are highlighted.

### **2.1.6 Summary**

The application of a resolving DC signal appears to be the prevailing method for single notch isolation with a resolution of  $\sim 100$ , which is sufficient to isolate individual charge states of native and denatured monoclonal antibodies (mAbs) without losses. MS3 experiments involving isolation of mAb fragments subjected to an additional step of ion activation have been performed successfully using a resolving DC applied in segment Q2.

A new software module has been developed for calibrating ion secular frequencies. This new tool will be used to generate frequency calibration tables and greatly simplify the process of ion isolation. All calculations will be performed in the background and in an automated manner. In combination with the new USB3 communication port, which has been fully developed and tested, including all the necessary upgrades in VHDL and upper level software, these developments will allow the instrument to operate in data dependent acquisition mode and make it compatible with front-end separation methods.